ACCOUNTS
of chemical research

Exciton Fine Structure and Spin Relaxation in Semiconductor Colloidal Quantum Dots

JEONGHO KIM, CATHY Y. WONG, AND GREGORY D. SCHOLES*
Department of Chemistry, 80 St. George Street, Institute for Optical Sciences, and Center for Quantum Information and Quantum Control, University of Toronto, Ontario, M5S 3H6 Canada

RECEIVED ON SEPTEMBER 17, 2008

CONSPECTUS

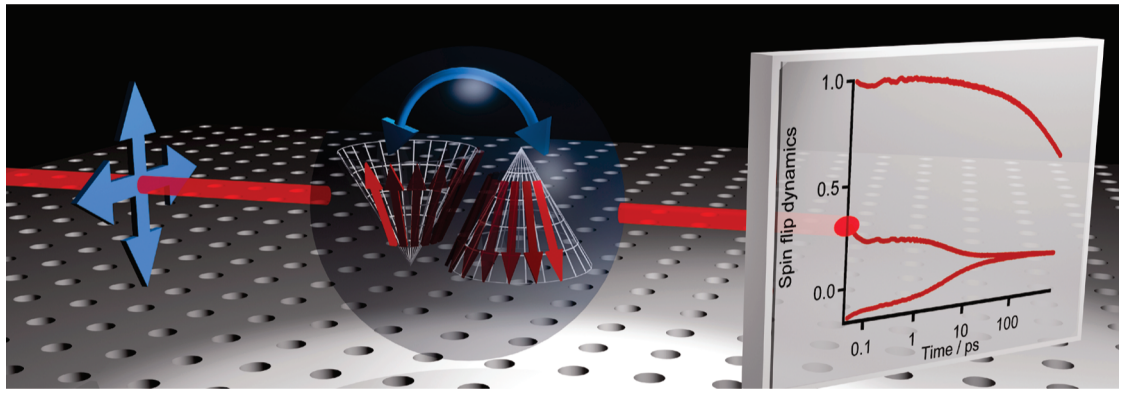

Quantum dots (QDs) have discrete quantum states isolated from the environment, making QDs well suited for quantum information processing. In semiconductor QDs, the electron spins can be coherently oriented by photoexcitation using circularly polarized light, creating optical orientation. The optically induced spin orientation could serve as a unit for data storage and processing. Carrier spin orientation is also envisioned to be a key component in a related, though parallel, field of semiconductor spintronics. However, the oriented spin population rapidly loses its coherence by interaction with the environment, thereby erasing the prepared information. Since long-lasting spin orientation is desirable in both areas of investigation, spin relaxation is the central focus of investigation for optimization of device performance.

In this Account, we discuss a topic peripherally related to these emerging areas of investigation: exciton fine structure relaxation (EFSR). The radiationless transition occurring in the exciton fine structure not only highlights a novel aspect of QD exciton relaxation but also has implications for carrier spin relaxation in QDs. We focus on examining the EFSR in connection with optical spin orientation and subsequent ultrafast relaxation of electron and hole spin densities in the framework of the exciton fine structure basis.

Despite its significance, the study of exciton fine structure in colloidal QDs has been hampered by the experimental challenge arising from inhomogeneous line broadening that obscures the details of closely spaced fine structure states in the frequency domain. In this Account, we show that spin relaxation occurring in the fine structure of CdSe QDs can be probed by a time-domain nonlinear polarization spectroscopy, circumventing the obstacles confronted in the frequency-domain spectroscopy. In particular, by combining polarization sequences of multiple optical pulses with the unique optical selection rules of semiconductors, fast energy relaxation among the QD exciton fine structure states is selectively measured. The measured exciton fine structure relaxation, which is a nanoscale analogue of molecular radiationless transitions, contains direct information on the relaxation of spin densities of electron and hole carriers, that is, spin relaxation in QDs.

From the exciton fine structure relaxation rates measured for CdSe nanorods and complex-shaped nanocrystals using nonlinear polarization spectroscopy, we elucidated the implications of QD size and shape on the QD exciton properties as well, for example, size- and shape-scaling laws governing exciton spin flips and how an exciton is delocalized in a QD. We envision that the experimental development and the discoveries of QD exciton properties presented in this Account will inspire further studies toward revealing the characteristics of QD excitons and spin relaxation therein, for example, spin relaxation in QDs made of various materials with different electronic structures, spin relaxation under an external perturbation of QD electronic states using magnetic fields, and spin relaxation of separated electrons and holes in type-II QD heterostructures.

Published on the Web 05/08/2009 www.pubs.acs.org
10.1021/ar8002046 CCC: $71.50

Introduction

Semiconductor quantum dots (QDs) are zero-dimensional structures with nanometer-scale size in all three axes.[1−5] The quantum confinement results in correlated behavior of electron−hole pair (exciton) and size-tunable discrete electronic states. Such a material can have many potential applications, including spintronics and quantum information processing.[6,7] The former utilizes both the spin and charge of carriers for information transport in electronic devices, and the latter involves the use of quantum mechanical systems for performing data operations. Both applications can make use of optical spin orientation coherently prepared in well-defined electronic states of suitably oriented QDs by photoexcitation using circularly polarized light. A problem facing researchers is that the oriented spin population rapidly loses its coherence by interaction with the environment, thereby erasing the prepared information. Thus, understanding decoherence of oriented spin states, i.e., spin relaxation, is a focus of investigation for these fields.

The topic of the present review is related to these emerging areas of investigation, but as we attempt to show, it has its own questions and challenges. This is the study of exciton fine structure relaxation (EFSR) that occurs in the fine structure of the lowest exciton in colloidal QDs. This dynamic phenomenon not only highlights novel aspects of QD exciton relaxation processes but also has implications for carrier spin relaxation in QDs. This Account focuses on examining the EFSR in connection with optical spin orientation and subsequent relaxation of electron and hole spin densities in the framework of the exciton fine structure basis. By considering the total angular momentum of each fine structure state and how that relates to the spin density of the electron and hole in the wave function, we associate EFSR with carrier spin relaxation. We describe the experimental method we have developed for studying EFSR, an approach that demonstrates the enormous potential of polarized optical pulse sequences in nonlinear spectroscopy.

QDs can be broadly classified into two types: epitaxially grown self-assembled QDs and colloidal nanocrystalline QDs. The self-assembled QDs have numerous advantages in spin device applications, namely, that they are oriented in one direction, which is well suited for optical generation of spin orientation, and that their placement in a substrate makes them easily incorporated into electronic devices. Due to such advantages of self-assembled QDs, a large body of work investigating the exciton fine structure and spin relaxation dynamics in self-assembled QDs have been reported.[8−15] However, the self-assembled QDs have many drawbacks as well, for example, difficulty in positioning the QDs on the substrate with high precision, limitation in precise shape control, and weak confinement owing to the size and properties of the wetting layer, etc.[16]

In contrast, many of these shortcomings are absent in colloidal QDs. Recent advances in wet-chemistry synthesis of colloidal QDs allow routine preparation of QDs of various sizes, shapes, and composition with narrow size distribution and strong confinement.[17−19] Considering the differences between the two types of QDs in their morphologies, orientations, and surrounding substrates, it cannot be readily assumed that the spins in colloidal QDs will behave in the same way as in their counterpart. Especially, colloidal QDs are randomly oriented in the host medium, so that a different approach for controlling and probing spin coherence is called for. In order to investigate the spin relaxation dynamics in colloidal QDs, the photophysics of these systems needs to be better understood. Here, we emphasize that this Account is concerned with spin relaxation occurring in the fine structure of colloidal QDs. Accordingly, from now on, we will refer to colloidal QDs as "QDs".

QD Exciton Fine Structure

Owing to the small size of QDs, the electron and hole are confined together, and treatments of the electron and hole as a single exciton quasiparticle have been shown to be accurate and practical. This confinement also results in significant contribution of the electron−hole exchange interaction to the electronic structure. In molecules, the exchange interaction causes the splitting of degenerate electron−hole pair configurations into singlet and triplet states. In comparison to singlet−triplet exchange splitting in molecules (∼1 eV) and in bulk semiconductors (<1 meV), an intermediate case is presented in QDs (1−25 meV). Owing to stronger spin−orbit coupling in QDs, it is total angular momentum (instead of spin) that is a good quantum number. The states in the QD fine structure are conveniently labeled by their projected total angular momentum, F, on the unique crystalline c-axis. In the molecular orbital picture, an excited electron is in an s-type orbital, and so $F_{electron}$ is $\pm 1/2$, while for a hole, in a p-type orbital, F_{hole} is $\pm 3/2$ or $\pm 1/2$. When an electron−hole pair is considered, F can have any integer value between $+2$ and -2. The lowest excitonic state of CdSe QDs consists of eight fine structure states, two with $F = \pm 2$, four with $F = \pm 1$ and two with $F = 0$.

As in molecules, the exchange interaction in QDs splits the lowest exciton state into two energy levels: the higher energy level with a total angular momentum of 1 (and thus $F = \pm 1$

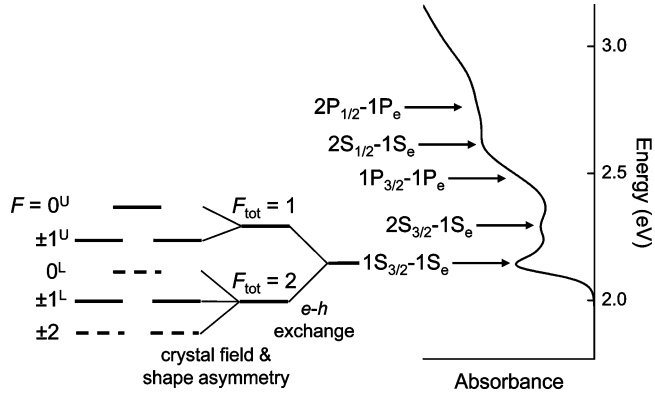

FIGURE 1. Optical absorption spectrum of colloidal CdSe QDs. Its absorption features are described in terms of excitons. The lowest exciton state, $1S_{3/2}-1S_e$, is split to the exciton fine structure by electron−hole exchange interaction, crystal field, and shape asymmetry. Each fine structure state is identified by its projected total angular momentum, *F*, obtained by mixing the total angular momenta of electron and hole.

or 0) and the lower energy level with a total angular momentum of 2 (with $F = \pm2$, ±1, or 0).[20,21] Since a photon cannot carry an angular momentum of 2, the $F = \pm2$ states are optically dark within the electric dipole approximation, while the states with $F = \pm1$ and 0 can be either dark or bright. To distinguish between these states, they can be referred to as upper ($F = \pm1^U$, 0^U) or lower ($F = \pm1^L$, 0^L). Aside from exchange interaction, other intrinsic effects can cause further splitting of the fine structure states. In particular, the intrinsic asymmetry in the crystal field of wurtzite CdSe QDs and QD shape asymmetry split the valence band into two energy levels, depending on the *F* value for the hole: the lower and higher energy states with $F_{hole} = \pm3/2$ and $F_{hole} = \pm1/2$, respectively.[21] When the effects of the electron−hole exchange interaction and valence band splitting due to asymmetry in the crystal field and the overall QD shape are all taken into consideration, the resulting fine structure has five energy levels, with three dark states ($F = \pm2$ and 0^L) and five bright states ($F = \pm1^U$, $\pm1^L$ and 0^U), as shown in Figure 1. Theory has predicted how the spacing and ordering of these states depends on confinement, crystal structure, and shape asymmetry.[21−23]

Relative to well-studied relaxation processes in QDs, such as radiative exciton recombination and Auger relaxation, the relaxation dynamics within the exciton fine structure have been studied to a lesser extent. The experimental investigation of the fine structure proves to be challenging because the size distribution of colloidal QDs introduces significant inhomogeneous broadening to optical spectra, effectively hiding the fine structure. Many experimental techniques have been used to overcome the obstacle of inhomogeneous broadening to study the fine structure. In particular, fluorescence line narrowing and photoluminescence excitation, which can selectively access a small subset of the QD ensemble, have been the most effective tools in probing the exciton fine structure. The studies using these techniques have successfully resolved the magnitude and size dependence of fine structure splitting and revealed that the band edge-emitting state is a dark state.[20,21,24,25] In contrast to these frequency-domain techniques, the cross-polarized, heterodyne detected third-order transient grating (CPH-3TG) method described in this Account is effective in selectively probing fast dynamic phenomena in the fine structure because the signal decay is induced when particular EFSR transitions occur, those that change the total angular momentum of the exciton.

Transient Polarization Grating and Exciton Fine Structure Relaxation

Spectroscopy using polarized light is a tool capable of probing the electronic structure of molecules, bulk materials, and nanoscale materials. By controlling the number of light−matter interactions and the polarizations of each light pulse in sequence, nonlinear polarization spectroscopy is able to provide information that is not available in linear spectroscopy. For example, transient (population) grating and polarization grating techniques use a sequence of three ultrafast laser pulses to initiate and probe dynamics. The probe step involves interrogation with the third pulse in the sequence, but the information is obtained in a unique fourth direction as the third-order polarization radiated by the sample. We measure that signal using heterodyne detection, whereby a fourth extra pulse is mixed with the signal interferometrically to allow phase-sensitive detection of the signal electric field amplitude. Generally speaking, transient grating measures population decay, whereas polarization grating measures depolarization. The utility of these experiments is based on the concept that optical selection rules for systems being probed in an isotropic ensemble can be more effectively probed or utilized in higher order nonlinear optical experiments. That is because the signal in such experiments arises from multiple probing of each molecule, and each of those probe steps can happen with a polarization and geometry chosen by the experimenter. Essentially, one has more opportunity to fine-tune the polarization selection, which is mathematically represented by the size and structure of the isotropic Cartesian tensor that relates the laboratory-frame polarizations to the transition moment vector (or nonlinear response tensor) in the molecular frame.[26−28]

The spectroscopic method of CPH-3TG offers a means to probe ultrafast dynamics among the nearly degenerate QD

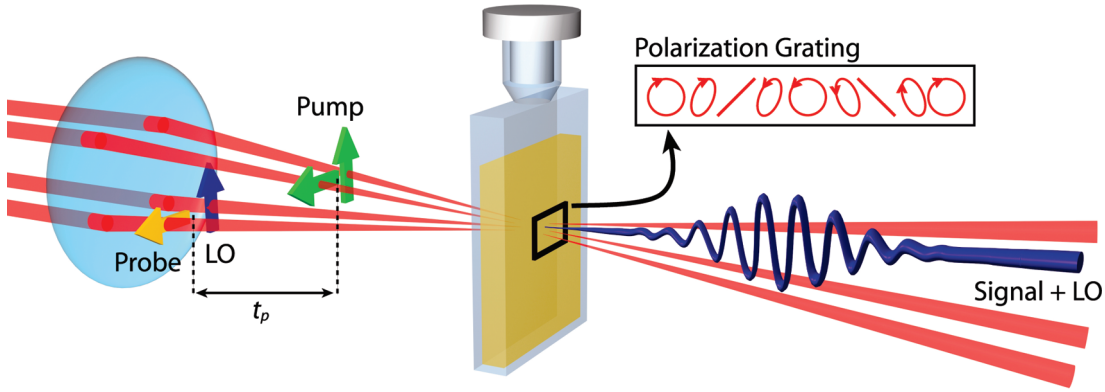

FIGURE 2. Schematic of CPH-3TG experiment. At the sample, polarization grating is formed by the interaction of two cross-linearly polarized pump pulses (green arrows). As a result, a spatially modulated pattern of polarizations between right-circular, 45° linear, left-circular, and −45° linear polarizations is formed in a plane. In particular, the pattern of alternating right- and left-circular polarization, forming a spin grating, is emphasized in this work. A time-delayed probe pulse (yellow arrow) is diffracted off the grating to radiate the heterodyned third-order polarization signal into the propagation direction of the local oscillator (LO, blue arrow).

fine structure states.[29] In CPH-3TG, there are four polarizations that can be controlled/analyzed: the pump pulse pair, the probe, and the radiated polarization. It works based on selection rules of semiconductors for circularly polarized light, and the measured signal evolves according to a clever interference effect that enables us to measure the rate of processes that flip the sign of the exciton total angular momentum, F. Such angular momentum flips necessarily involve electron and/or hole spin flips. Notably, such selectivity is achieved without needing to excite a specific spin state using circularly polarized light to generate spin orientation. Instead, we measure a polarization tensor element that is sensitive to spin flip events in dynamic equilibrium between $F = +1, +2$ and $F = -1, -2$ exciton states.[30]

The schematic of the CPH-3TG experiment is shown in Figure 2. The CPH-3TG method makes use of the polarization grating that is formed by the interaction of two orthogonal linearly polarized light pulses. According to the crossing angle of the laser beams, the polarization is spatially modulated across the excitation region, leading to a periodic spatial pattern of right- and left-circular polarization,[31] as shown in Figure 2. The selection rules of wurtzite and zinc-blende semiconductors allow $F = +1$ or -1 excitons in suitably oriented QDs to be selectively excited by circularly polarized light depending on the handedness of circular polarization. Therefore, the polarization grating creates a pattern of angular momentum projections across the excitation volume. If the crystallographic c-axis of each QD was aligned in the laboratory frame, then this angular momentum grating would correspond to alternating $F = +1$ and -1 exciton states, which can be related to a spin grating.[32] Obviously the QDs in solution samples are not oriented, but their random orientation is accommodated in the theory for our experiment.[29] A time-delayed probe pulse interrogates the projected angular momentum grating and is diffracted, that is, it induces radiation of third-order transient grating (3-TG) signal. The third-order signal decays as the modulation pattern of the angular momentum projections becomes randomized by exciton fine structure relaxation. Thus, the CPH-3TG signal can monitor the history of spin flips between $F = +1$ and -1 exciton fine structure states in randomly oriented QDs without a need for circularly polarized excitation light.

The principle of the CPH-3TG method is theoretically described using third-order response functions and rotational averaging for an ensemble of colloidal QDs.[29,30] A schematic describing the principle of the CPH-3TG method from the perspective of third-order nonlinear spectroscopy is shown in Figure 3. After an exciton spin state (e.g., $F = +1$ state in Figure 3(a)) is excited by the interactions with two cross-polarized pump pulses, the exciton can be either "conserved" or "flipped" in its spin (i.e., sign of F) at the moment it interacts with a probe pulse to radiate the third order polarization, $P^{(3)}$. At the initial moment when pump and probe pulses are coincident in time, the spins of all excitons stay conserved since there is no time for a spin flip to occur. As the time delay between pump and probe pulses increases, the number of excitons with flipped spins increases until the numbers of excitons with conserved and flipped spins, n_C and n_F, respectively, equilibrate. By rotationally averaging the third-order responses over an ensemble of randomly oriented QDs, it was found that the electric field of radiated $P^{(3)}$ changes its phase by π depending on whether the exciton spin is "conserved" or "flipped" at the probing moment, Figure 3(b). As a result, the $P^{(3)}$ radiated from spin-conserved and flipped excitons interfere destructively to induce the decay of the resultant 3-TG signal. Here, it should be noted that the ensemble populations of $F = +1$

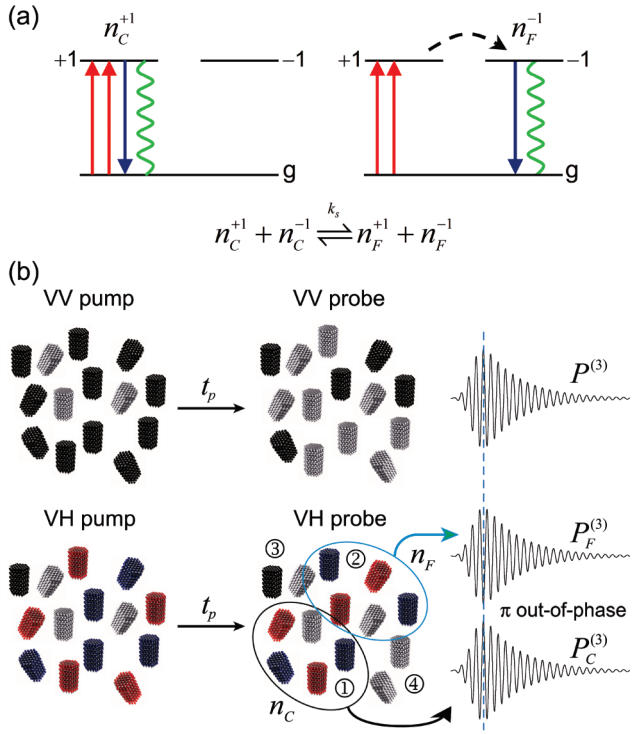

FIGURE 3. (a) Two cross-polarized pump pulses (red arrows) excite $F = +1$ or $F = -1$ exciton spin state with an equal ratio; after a time delay, t_p, a probe pulse (blue arrow) interacts to radiate the third-order polarization (green wavy line). At the probing moment, the exciton spin is either conserved (left) or flipped (right). (b) Schematic of 3-TG experiment on QDs with various polarization sequences. Top: VVVV 3-TG experiment. Nanorod ensemble is in either an excited (black) or the ground (silver) state. The amplitude of the radiated polarization, $P^{(3)}$, is proportional to the number of nanorods in the excited state. Bottom: VHVH 3-TG experiment. Nanorods are photoexcited to $F = 0$ (black), $F = +1$ (red), and $F = -1$ (blue) excitons. The electric fields of radiated third-order polarization from (1) conserved ($P_C^{(3)}$) and (2) flipped ($P_F^{(3)}$) excitons are different in phase by π, thus interfering destructively to induce the signal decay. Meanwhile, nanorods (3) with $F = 0$ excitons and (4) that relax back to the ground state radiate polarization of the same phase as the VVVV signal. Adapted and reproduced from ref 38.

and -1 exciton spin states always stay equal after excitation by two cross-polarized pump pulses.

Measurement of Exciton Fine Structure Relaxation and Spin Relaxation

The heterodyned 3-TG signal is measured by an experimental setup using a diffractive optic, of which the details are described elsewhere.[30] The 3-TG signals of QDs are recorded with VVVV, VHVH, and VHHV polarization sequences, where V and H represent the vertical and horizontal polarizations, respectively, of the two pump beams, a probe beam, and an analyzer in order. Representative 3-TG signals of QDs measured with these polarization sequences are shown in Figure 4(a). The VVVV signal exhibits a slow decay on the time scale

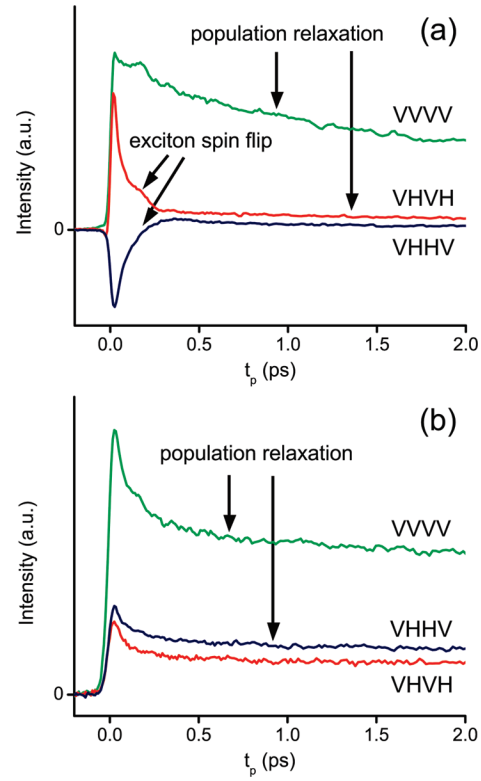

FIGURE 4. The 3-TG signals of (a) CdSe QDs (2.7 nm diameter) and (b) laser dye (Rhodamine 6G) measured with VVVV, VHVH, and VHHV polarization sequences. Spin relaxation dynamics in the VHVH and VHHV signals are observed only in QDs, distinguished from population relaxation dynamics. The sub-100 fs decay component in the 3-TG signals of laser dye is ascribed to coherent artifact, not sample response, arising from the temporal overlap of three light pulses. Adapted and reproduced from ref 30.

ranging from tens of picoseconds to nanoseconds. It reflects the dynamics of exciton population relaxation, as measured with a conventional pump−probe experiment. In contrast, the VHVH and VHHV signals initially decay much faster than the VVVV signal, followed by a slow decay equivalent to the VVVV signal. This fast decay arises as the excitons flip their spins via population transfer between the $F = +1$ and -1 states. The opposite signs in the initial amplitudes of the VHVH and VHHV signals support this assignment since theory predicts that the two cross-polarized signals show oppositely signed rotational averaging factors.[30] Once equilibrium is reached between the numbers of conserved and flipped exciton spins, the two CPH-3TG signals converge and decay slowly as the exciton population relaxes down to the ground state. The rate of exciton spin flip can be obtained by multiexponential fitting of the measured 3-TG signals.

For comparison, the 3-TG signal measured for a laser dye, Rhodamine 6G, is shown in Figure 4(b). Both VHVH and VHHV signals are equivalent to each other in their sign, and they decay with dynamics similar to the VVVV signal, with the only

difference being their relative amplitude. Thus, it is evident that the cross-polarized 3-TG signals for QD samples are a special case.

It should be noted that exciton population relaxation represented by the VVVV signal is affected by trapping at surface states, as manifested by a fast decay component on the order of several picoseconds in Figure 4(a). This fast decay is not associated with multiexciton Auger process since the number of excitons per dot was kept much lower than 1 in our measurements. However, the surface trap states do not influence the spin flip rate extracted from cross-polarized signals, as was confirmed by identical spin flip rates obtained for freshly synthesized and aged QDs (1 year).

To understand the mechanism of spin flips in colloidal QDs, an analysis was made using a kinetic model that includes all the states in the exciton fine structure, as shown in Figure 5(a). The kinetic model uses coupled equations of motion to determine the transient populations of each fine structure state so that the spin flip history of excitons can be monitored, as detailed elsewhere.[33] While the ordering of the fine structure states is sensitive to the size and aspect ratio of a QD,[23,34,35] the exciton fine structure ordering of spherical QDs was used for kinetic analysis of our data. Although cylindrical nanorods were investigated as well, which will be discussed below, all nanorod samples lie in the size and aspect ratio regime where the fine structure ordering of spherical QDs is maintained.[23] The 3-TG signals arising from various polarization sequences were simulated to fit the experimental data for QDs, and kinetic parameters for transitions among the fine structure states were obtained. Examples of simulated 3-TG signals using this kinetic analysis are shown in Figures 5(b) and 5(c), where each transition in the fine structure is assigned to a 3-TG signal decay component on an appropriate time scale. Although EFSR occurs by the complex interplay of all the fine structure states as manifested by the multiexponential decay of 3-TG signals, our analysis suggests that the dominant relaxation pathway is the $F = +1^{L} \rightarrow -2$ transition or equivalently $F = -1^{L} \rightarrow +2$ transition (**a** in Figure 5).

The electron and hole spin densities of each fine structure state can be calculated from the eigenstate configurations comprising each state, and therefore the kinetics of EFSR can be translated into spin relaxation dynamics.[36] As an example, the simulation results using the kinetic parameters obtained from our experimentally measured CPH-3TG signals are shown in Figure 6. From the population evolution of the fine structure states, time-dependent changes in electron and hole spin densities of α (spin-up) and β (spin-down) spins are retrieved. This result exemplifies that the relaxation dynamics of spin densities can be obtained from population relaxation dynamics in the exciton fine structure. It can be seen that

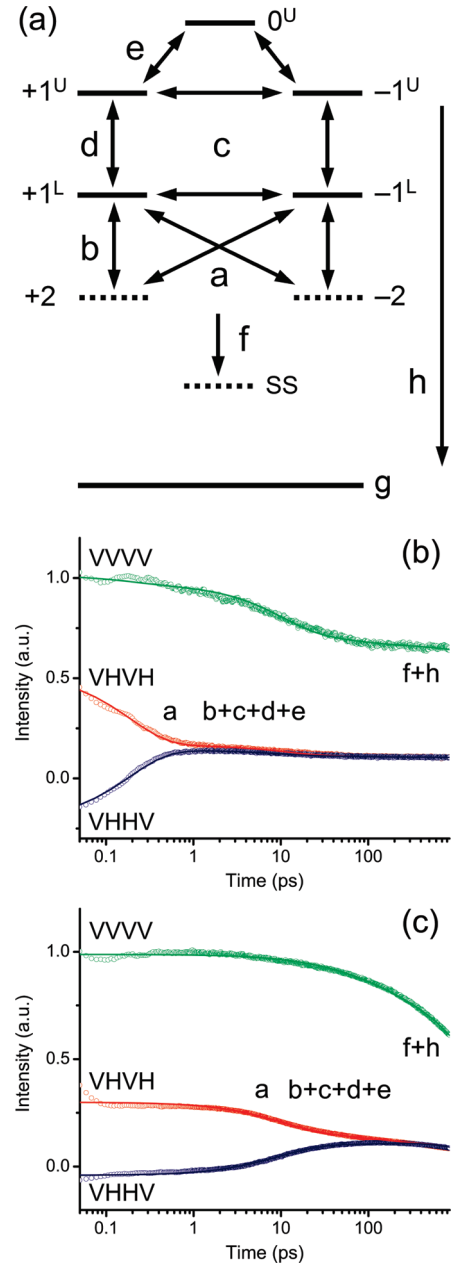

FIGURE 5. (a) Kinetic model of relaxation in the exciton fine structure considering all the transitions between fine structure states. The possible transitions between the fine structure states are depicted as arrows. The simulated signals (solid line) using the kinetic model are compared with 3-TG signals (empty circles) experimentally measured for nanorods of (b) 3.6 nm and (c) 8.4 nm diameter. The transition, **a**, is the dominant process that gives rise to the fastest decay of VHVH and VHHV signals. Subsequently, the interplay of **b**, **c**, **d** and **e** gives rise to the second decay component of the cross-polarized signals, more notably in the larger nanorod in (c). In contrast, the decays of VVVV signal and the slowest decay component of VHVH and VHHV signals are dominated by slow relaxation processes to the surface states (SS), **f**, and to the ground state (g), **h**, on nanosecond time scale.

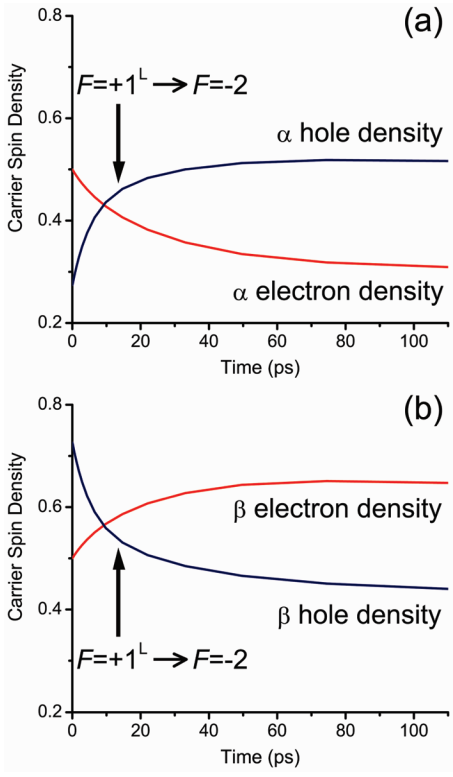

FIGURE 6. Time evolutions of carrier spin densities of (a) α (spin-up) and (b) β (spin-down) spin parities simulated using the kinetic fitting parameters obtained from our experimentally measured 3-TG data shown in Figure 6(c). In this simulation, only $F = +1^{L}$, $F = +1^{U}$, and $F = 0^{U}$ states are initially photoexcited. It should be noted that α and β spin densities change in an anticorrelated manner to each other. The changes of the hole spin densities are faster than those of the electron spin densities, corresponding to the dominant $F = +1^{L} \rightarrow F = -2$ relaxation pathway.

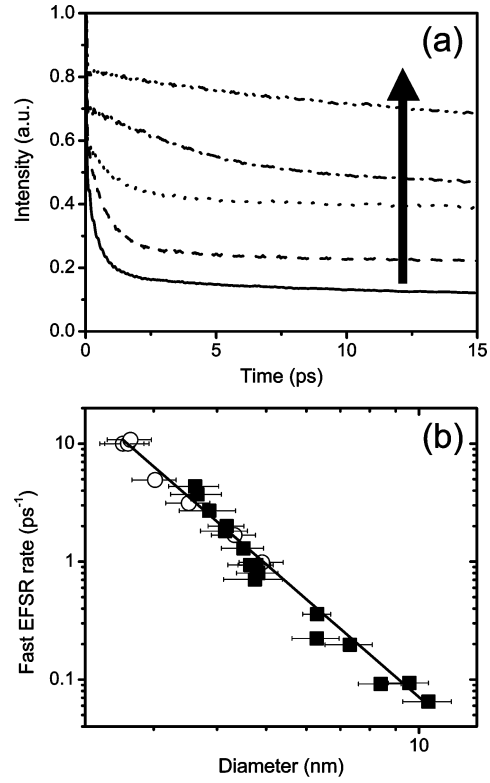

FIGURE 7. (a) The CPH-3TG signals measured for various sizes and shapes of nanorods. The spin flip decay becomes slower as the nanorod diameter increases (from bottom to top), as indicated by a black arrow. (b) Plot of EFSR rate versus diameter of nanorods (filled square) and QDs (open circle). The data points were fitted with $1/d^4$ power law fit (solid line). Adapted and reproduced from ref 36.

the fast CPH-3TG signal decay arising from the dominant $F = +1^{L} \rightarrow -2$ relaxation pathway is attributed to the spin density decay of the hole rather than the electron component of the exciton wave function.

Size and Shape Dependence of Exciton Fine Structure Relaxation

The effect of QD size and shape on optoelectronic properties has been a major theme in recent QD research. The QD size effect is already well demonstrated by the size-dependent "bandgap" emission.[37] However, bandgap emission is not enough to reveal the subtle effect of QD size and shape on the electronic structure of QD excitons because such emission is mainly determined by large bandgap energy rather than the intricate interactions governing QD exciton properties. More detailed information about QD excitons can be provided by looking into the exciton fine structure, which is tuned by small interactions arising from quantum mechanical effects.

We examined QD size and shape effects on the spin flip rate by measuring CPH-3TG signals of CdSe QDs and nanorods of various sizes and shapes.[33,38] As can be seen in Figure 7(a), the decay profile of cross-polarized 3-TG signals varies depending on the size of CdSe nanorods. In general, the spin flip decay becomes slower as the diameter of nanorod increases. Also, an extra spin flip decay component was observed in large-sized nanorods, yielding biexponential spin relaxation dynamics with time constants of k_{s1} (fast) and k_{s2} (slow). In order to systematically analyze the relationships between exciton spin flip rates and the physical size and shape of nanorods, the dependence of exciton spin flip rates was examined versus various nanorod shape parameters such as diameter (short-axis dimension of a cylindrical nanorod), length, volume, and aspect ratio.

Remarkably, the fast exciton spin flip rate, k_{s1}, of spherical QDs and cylindrical nanorods shows a strong correlation only with the diameter of the nanorod rather than other shape parameters, Figure 7(b). As a consequence, nanorods of very different shapes show similar fast spin flip rates as long as their diameters are similar to each other. The diameter depen-

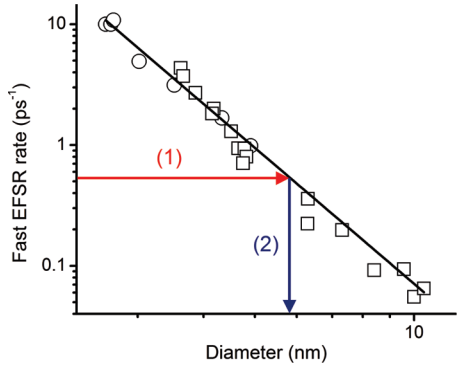

FIGURE 8. Determination of exciton size using the empirical calibration curve. (1) The fast EFSR rate of a nanocrystal sample is determined from the CPH-3TG measurement. (2) Then, the size of an exciton confined in a measured nanocrystal can be determined by comparing the rate with the $1/d^4$ relationship (solid line) obtained from the data points of CdSe spherical QDs (circles) and nanorods (squares).

dence of the exciton spin flip rate is well fit by a $1/d^4$ power law shown as a solid line in Figure 7(b). This relationship suggests a scaling law for the matrix element governing exciton spin flip transitions. In other words, it is the confinement in the plane perpendicular to the *c*-axis that determines the matrix element governing the fast exciton spin flip. In contrast to the strong diameter dependence of the fast exciton spin flip rate, no clear size dependence was found for the slow exciton spin flip rate, k_{s2}, which was observed only in QDs larger than 4.5 nm diameter. The physical origin of these spin flip transitions and their size dependence are discussed in detail in ref 36.

The $1/d^4$ scaling relationship obtained from the exciton spin flip rates of spherical QDs and nanorods can serve as an empirical calibration curve to determine the effective size of an exciton confined in a QD. Based on this idea, we examined the exciton size and exciton delocalization properties in complex-shaped nanocrystals.[39] The exciton size confined in such nanocrystals was estimated by comparing the measured exciton spin flip rate with the $1/d^4$ calibration curve, as shown in Figure 8. This study revealed the subtle influence of QD shape on the exciton properties, demonstrating that the overall physical shape of a QD does matter in determining the size and shape of the confined exciton.

Conclusion and Future Outlook

In this Account, we demonstrated that the CPH-3TG method provides a means of probing ultrafast relaxation dynamics occurring in the exciton fine structure in randomly oriented colloidal QDs. By applying the technique to different sizes and shapes of CdSe QDs, we learned the implications of QD size and shape for the QD exciton properties as well as the mechanism and origin of the relaxation processes accompanying exciton spin flip phenomena.

The spin relaxation dynamics of colloidal QDs can be compared with previous studies, mostly for self-assembled QDs, using time-resolved Faraday rotation technique[40,41] and time-resolved photoluminescence with circularly polarized light.[42,43] In both techniques, spin orientation is optically created in suitably oriented QDs by circularly polarized photoexcitation and subsequent relaxation of the spin orientation is manifested as the decay of their signals. This is in contrast to the working principle of CPH-3TG, whereby up- and down-spins are equally generated by a combination of cross-linearly polarized light, even in randomly oriented QDs. However, all these techniques are common in that the spin relaxation dynamics of different carriers are extracted from multiexponential decay of the measured signals. The fast spin flip time measured at room temperature in our studies is comparable to the hole spin relaxation time on the order of tens of picoseconds measured at low temperature in more weakly confined self-assembled QDs.[42,43] In contrast to hole spins, electron spin relaxation is much slower, on the nanosecond time scale,[40−43] and it can be further extended up to millisecond time scale by laser cooling of a charged QD.[14,15] The slow spin flip time on the order of hundreds of picoseconds to nanoseconds measured in our experiments is comparable to the electron spin relaxation time, considering that all of our measurements were done at room temperature. In general, the spin relaxation times vary considerably depending on the temperature, type of QDs (self-assembled or colloidal, charged or neutral), type of carrier of interest (electron, hole, exciton), and external perturbation (external magnetic field, charging of QDs), making direct comparison between the studies difficult. More detailed comparison with other studies will be discussed elsewhere.[44]

The development of the CPH-3TG technique should inspire studies to further elucidate the characteristics of nanoscale excitons in QDs. For example, this technique can be applied to QDs made of different materials, such as lead salt QDs,[45] to investigate how different exciton fine structure, for example, the ordering and degeneracies of fine structure states and the magnitude of spin−orbit interactions, influences spin relaxation. The CPH-3TG measurement can be combined with an external perturbation of the QD electronic states. In particular, when a strong external magnetic field is applied, the energy spacing between fine structure states changes[46] and dark states are mixed with bright states and gain oscillator strength.[21] Such perturbations in the fine structure will acti-

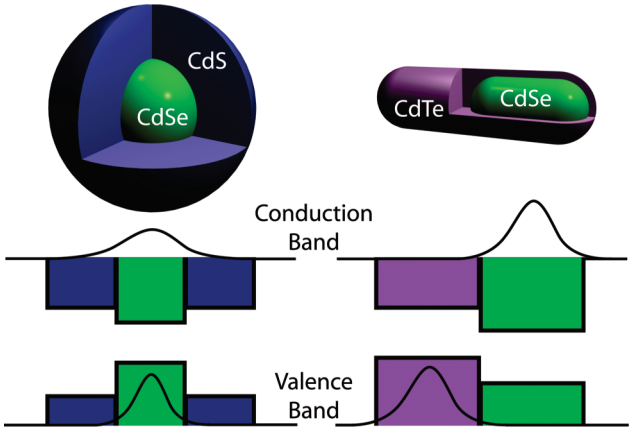

FIGURE 9. Schematic of QD type-II heterostructure along with typical profiles of the valence and conduction band confinement potentials. The curves in the valence and conduction bands indicate the probability distributions of hole and electron, respectively. (Left) CdSe/CdS core/shell QD: the hole is localized in the CdSe core, while the electron is delocalized over core and shell. (Right) CdSe/CdTe heterostructure nanorod: the hole and electron are localized in CdTe and CdSe rods, respectively, leading to charge separation.

vate (or deactivate) certain relaxation pathways, thus providing the prospect of controlling the mechanism of spin relaxation.

By tuning the electronic structure of QDs in more significant ways, control of exciton fine structure relaxation might be possible. QD type II heterostructures have become available with advances in nanocrystal synthesis.[47,48] These systems can be designed to allow the experimenter to photoexcite an exciton that rapidly separates into an electron and hole, Figure 9. This charge separation occurs at the interface of the two materials, for example CdSe and CdTe. By measuring spin relaxation dynamics of these separated electron and hole carriers, one can more clearly elucidate the mechanism of spin relaxation and thus learn how to orient and preserve carrier spins. This has just recently been demonstrated in a recent work from our laboratory.[49]

We thank the Natural Science and Engineering Research Council of Canada for the financial support of this research.

BIOGRAPHICAL INFORMATION

Jeongho Kim received his B.Sc. degree in chemistry from Korea Advanced Institute of Science and Technology. Then, he earned his M.S. and Ph.D. degrees in chemistry from the University of Chicago under the advisement of Prof. Norbert Scherer. Upon graduating in 2004, he moved to the University of Toronto as a postdoctoral fellow under Prof. Gregory Scholes. His major research interests are to investigate the fast dynamics in the excited electronic states of molecular systems and nanoscale materials using ultrafast nonlinear spectroscopy.

Cathy Wong completed her B.Sc. in Biological Chemistry at McMaster University and is currently a graduate student in the laboratory of Greg Scholes. Her research focuses on investigating the exciton dynamics of semiconductor nanocrystals using ultrafast spectroscopy and theory.

Gregory Scholes is an Associate Professor at the University of Toronto in the Department of Chemistry. He joined the faculty there in 2000. He obtained B.Sc. (Hons.) (1990) and Ph.D. (1994) degrees from the University of Melbourne, then undertook postdoctoral studies at Imperial College in London from 1995 to 1997 as a Ramsay Memorial Research Fellow and at the University of California, Berkeley, from 1997 to 2000. He is presently an NSERC EWR Steacie Fellow. His present research focuses on elucidating the principles deciding electronic structure, optical properties, and reactions of nanoscale systems by combining synthesis, theory, and ultrafast laser spectroscopy.

FOOTNOTES

*To whom correspondence should be addressed. E-mail: gscholes@chem.utoronto.ca.

REFERENCES

1 Bawendi, M. G.; Steigerwald, M. L.; Brus, L. E. The quantum mechanics of larger semiconductor clusters (quantum dots). *Annu. Rev. Phys. Chem.* **1990**, *41*, 477–496.

2 Weller, H. Colloidal semiconductor Q-particles: Chemistry in the transition region between solid state and molecules. *Angew. Chem., Int. Ed.* **1993**, *32*, 41–53.

3 Alivisatos, A. P. Perspectives on the physical chemistry of semiconductor nanocrystals. *J. Phys. Chem.* **1996**, *100*, 13226–13239.

4 Burda, C.; Chen, X. B.; Narayanan, R.; El-Sayed, M. A. Chemistry and properties of nanocrystals of different shapes. *Chem. Rev.* **2005**, *105*, 1025–1102.

5 Scholes, G. D. Controlling the optical properties of inorganic nanoparticles. *Adv. Funct. Mater.* **2008**, *18*, 1157–1172.

6 Elzerman, J. M.; Hanson, R.; Willems van Beveren, L. H.; Witkamp, B.; Vandersypen, L. M. K.; Kouwenhoven, L. P. Single-shot read-out of an individual electron spin in a quantum dot. *Nature* **2004**, *430*, 431–435.

7 Hanson, R.; Kouwenhoven, L. P.; Petta, J. R.; Tarucha, S.; Vandersypen, L. M. K. Spins in few-electron quantum dots. *Rev. Mod. Phys.* **2006**, *79*, 1217–1265.

8 Blackwood, E.; Snelling, M. J.; Harley, R. T.; Andrews, S. R.; Foxon, C. T. B. Exchange interaction of excitons in GaAs heterostructures. *Phys. Rev. B* **1994**, *50*, 14246–14254.

9 Ivchenko, E. L. Fine structure of excitonic levels in semiconductor nanostructures. *Phys. Status Solidi A* **1997**, *164*, 487–492.

10 Bayer, M.; Ortner, G.; Stern, O.; Kuther, A.; Gorbunov, A. A.; Forchel, A.; Hawrylak, P.; Fafard, S.; Hinzer, K.; Reinecke, T. L.; Walck, S. N.; Reithmaier, J. P.; Klopf, F.; Schafer, F. Fine structure of neutral and charged excitons in self-assembled In(Ga)As/(Al)GaAs quantum dots. *Phys. Rev. B* **2002**, *65*, 195315.

11 Maialle, M. Z.; de Andrada e Silva, E. A.; Sham, L. J. Exciton spin dynamics in quantum wells. *Phys. Rev. B* **1993**, *47*, 15776–15788.

12 Vinattieri, A.; Shah, J.; Damen, T. C.; Kim, D. S.; Pfeiffer, L. N.; Maialle, M. Z.; Sham, L. J. Exciton dynamics in GaAs quantum wells under resonant excitation. *Phys. Rev. B* **1994**, *50*, 10868–10879.

13 Gammon, D.; Snow, E. S.; Shanabrook, B. V.; Katzer, D. S.; Park, D. Fine structure splitting in the optical spectra of single GaAs quantum dots. *Phys. Rev. Lett.* **1996**, *76*, 3005–3008.

14 Atature, M.; Dreiser, J.; Badolato, A.; Hogele, A.; Karrai, K.; Imamoglu, A. Quantum-dot spin-state preparation with near-unity fidelity. *Science* **2006**, *312*, 551–553.

15 Gerardot, B. D.; Brunner, D.; Dalgarno, P. A.; Ohberg, P.; Seidl, S.; Kroner, M.; Karrai, K.; Stoltz, N. G.; Petroff, P. M.; Warburton, R. J. Optical pumping of a single hole spin in a quantum dot. *Nature* **2008**, *451*, 441–444.

16 Bryant, G. W. Quantum dots in quantum well structures. *J. Lumin.* **1996**, *70*, 108–119.

17 Murray, C. B.; Norris, D. J.; Bawendi, M. G. Synthesis and characterization of nearly monodisperse CdE (E = sulfur, selenium, tellurium) semiconductor nanocrystallites. *J. Am. Chem. Soc.* **1993**, *115*, 8706–8715.

18 Peng, X.; Manna, L.; Yang, W.; Wickham, J.; Scher, E.; Kadavanich, A.; Alivisatos, A. P. Shape control of CdSe nanocrystals. *Nature* **2000**, *404*, 59–61.

19 Yin, Y.; Alivisatos, A. P. Colloidal nanocrystal synthesis and the organic-inorganic interface. *Nature* **2005**, *437*, 664–670.

20 Chamarro, M.; Gourdon, C.; Lavallard, P.; Lublinskaya, O.; Ekimov, A. I. Enhancement of electron-hole exchange interaction in CdSe nanocrystals: A quantum confinement effect. *Phys. Rev. B* **1996**, *53*, 1336–1342.

21 Efros, A. L.; Rosen, M.; Kuno, M.; Nirmal, M.; Norris, D. J.; Bawendi, M. Band-edge exciton in quantum dots of semiconductors with a degenerate valence band: Dark and bright exciton states. *Phys. Rev. B* **1996**, *54*, 4843–4856.

22 Li, J.; Wang, L.-W. Shape effects on electronic states of nanocrystals. *Nano Lett.* **2003**, *3*, 1357–1363.

23 Zhao, Q.; Graf, P. A.; Jones, W. B.; Franceschetti, A.; Li, J.; Wang, Kim. K. Shape dependence of band-edge exciton fine structure in CdSe nanocrystals. *Nano Lett.* **2007**, *7*, 3274–3280.

24 Nirmal, M.; Norris, D. J.; Kuno, M.; Bawendi, M. G.; Efros, A. L.; Rosen, M. Observation of the "dark exciton" in CdSe quantum dots. *Phys. Rev. Lett.* **1995**, *75*, 3728–3731.

25 Kuno, M.; Lee, J. K.; Dabbousi, B. O.; Mikulec, F. V.; Bawendi, M. G. The band edge luminescence of surface modified CdSe nanocrystallites: Probing the luminescing state. *J. Chem. Phys.* **1997**, *106*, 9869–9882.

26 McClain, W. M. Polarization of two-photon excited fluorescence. *J. Chem. Phys.* **1973**, *58*, 324–326.

27 Wagniere, G. Optical activity of higher order in a medium of randomly oriented molecules. *J. Chem. Phys.* **1982**, *77*, 2786–2792.

28 Andrews, D. L.; Blake, N. P. Three-dimensional rotational averages in radiation-molecule interactions: an irreducible cartesian tensor formulation. *J. Phys. A: Math. Gen.* **1989**, *22*, 49–60.

29 Scholes, G. D. Selection rules for probing biexcitons and electron spin transitions in isotropic quantum dot ensembles. *J. Chem. Phys.* **2004**, *121*, 10104–10110.

30 Scholes, G. D.; Kim, J.; Wong, C. Y. Measurement of exciton spin relaxation in quantum dots using an ultrafast transient polarization grating spectroscopy. *Phys. Rev. B* **2006**, *73*, 195325.

31 Fourkas, J. T.; Trebino, R.; Fayer, M. D. The grating decomposition method: A new approach for understanding polarization-selective transient grating experiments. I. Theory. *J. Chem. Phys.* **1992**, *97*, 69–77.

32 Cameron, A. R.; Riblet, P.; Miller, A. Spin gratings and the measurement of electron drift mobility in multiple quantum well semiconductors. *Phys. Rev. Lett.* **1996**, *76*, 4793–4796.

33 Kim, J.; Wong, C. Y.; Nair, P. S.; Fritz, K. P.; Kumar, S.; Scholes, G. D. Mechanism and origin of exciton spin relaxation in CdSe nanorods. *J. Phys. Chem. B* **2006**, *110*, 25371–25382.

34 Hu, J.; Li, L.-S.; Yang, W.; Manna, L.; Wang, L.-W.; Alivisatos, A. P. Linearly polarized emission from colloidal semiconductor quantum rods. *Science* **2001**, *292*, 2060–2063.

35 Le Thomas, N.; Herz, E.; Schops, O.; Woggon, U. Exciton fine structure in single CdSe nanorods. *Phys. Rev. Lett.* **2005**, *94*, 016803.

36 Wong, C. Y.; Kim, J.; Nair, P. S.; Nagy, M. C.; Scholes, G. D. Relaxation in the exciton fine structure of semiconductor nanocrystals. *J. Phys. Chem. C* **2009**, *113*, 795–811.

37 Li, L.-S.; Hu, J.; Yang, W.; Alivisatos, A. P. Band gap variation of size- and shape-controlled colloidal CdSe quantum rods. *Nano Lett.* **2001**, *1*, 349–351.

38 Scholes, G. D.; Kim, J.; Wong, C. Y.; Huxter, V. M.; Nair, P. S.; Fritz, K. P.; Kumar, S. Nanocrystal shape and the mechanism of exciton spin relaxation. *Nano Lett.* **2006**, *6*, 1765–1771.

39 Kim, J.; Nair, P. S.; Wong, C. Y.; Scholes, G. D. Sizing up the exciton in complex-shaped semiconductor nanocrystals. *Nano Lett.* **2007**, *7*, 3884–3890.

40 Gupta, J. A.; Awschalom, D. D.; Peng, X.; Alivisatos, A. P. Spin coherence in semiconductor quantum dots. *Phys. Rev. B* **1999**, *59*, R10421—R10424.

41 Gupta, J. A.; Awschalom, D. D.; Efros, A. L.; Rodina, A. V. Spin dynamics in semiconductor nanocrystals. *Phys. Rev. B* **2002**, *66*, 125307.

42 Gundogdu, K.; Hall, K. C.; Koerperick, E. J.; Pryor, C. E.; Flatte, M. E.; Boggess, T. F.; Shchekin, O. B.; Deppe, D. G. Electron and hole spin dynamics in semiconductor quantum dots. *Appl. Phys. Lett.* **2005**, *86*, 113111.

43 Hall, K. C.; Koerperick, E. J.; Boggess, T. F.; Shchekin, O. B.; Deppe, D. G. Hole spin relaxation in neutral InGaAs quantum dots: Decay to dark states. *Appl. Phys. Lett.* **2007**, *90*, 053109.

44 Huxter, V. M.; Kim, J.; Lo, S. S.; Lee, A.; Nair, P. S.; Scholes, G. D. Spin relaxation in zinc blende and wurtzite CdSe quantum dots. *Synth. Met.*, submitted.

45 Johnson, J. C.; Gerth, K. A.; Song, Q.; Murphy, J. E.; Nozik, A. J. Ultrafast exciton fine structure relaxation dynamics in lead chalcogenide nanocrystals. *Nano Lett.* **2008**, *8*, 1374–1381.

46 Furis, M.; Htoon, H.; Petruska, M. A.; Klimov, V. I.; Barrick, T.; Crooker, S. A. Bright-exciton fine structure and anisotropic exchange in CdSe nanocrystal quantum dots. *Phys. Rev. B* **2006**, *73*, 241313.

47 Kim, S.; Fisher, B.; Eisler, H.-J.; Bawendi, M. G. Type-II quantum dots: CdTe/CdSe(core/shell) and CdSe/ZnTe(core/shell) heterostructure. *J. Am. Chem. Soc.* **2003**, *125*, 11466–11467.

48 Kumar, S.; Jones, M.; Lo, S. S.; Scholes, G. D. Nanorod heterostructures showing photoinduced charge separation. *Small* **2007**, *3*, 1633–1639.

49 He, J.; Lo, S. S.; Kim, J.; Scholes, G. D. Control of exciton spin relaxation by electron-hole decoupling in type-II heterostructures. *Nano Lett.* **2008**, *8*, 4007–4013.